View metadata, citation and similar papers at core.ac.uk
brought to you by CORE
provided by CERN Document Server

Negative parity states of ^{11}B and ^{11}C and the similarity with ^{12}C

Yoshiko Kanada-En'yo
Yukawa Institute for Theoretical Physics, Kyoto University, Kyoto 606-8502, Japan

The negative parity states of ^{11}B and ^{11}C were studied based on the calculations of antisymmetrized molecular dynamics(AMD). The calculations well reproduced the experimental strengths of Gamov-Teller(GT), $M1$ and monopole transitions. We, especially, focused on the $3/2^-_3$ and $5/2^-_2$ states, for which GT transition strengths were recently measured. The weak $M1$ and GT transitions for the $3/2^-_3$ in ^{11}B and ^{11}C are described by a well-developed cluster structure of 2α+t and 2α+^{3}He, respectively, while the strong transitions for the $5/2^-_2$ is characterized by an intrinsic spin excitation with no cluster structure. It was found that the $3/2^-_3$ state is a dilute cluster state, and its features are similar to those of the ^{12}C(0^+_2) which is considered to be a gas state of three α clusters.

arXiv:nucl-th/0612109v1 29 Dec 2006

I. INTRODUCTION

Cluster aspect is known to be one of essential features in light nuclei. Recently, various new types of cluster structure have been predicted and found in excited states of light stable nuclei as well as in light unstable nuclei. In case of ^{12}C, it was known that 3α-cluster states develop in such excited states as the 0^+_2(7.65 MeV) state. Tohsaki *et al.*[1, 2] proposed a new interpretation of the 0^+_2 as a dilute gas state of weakly interacting 3 α particles. It is challenging problem to answer the question whether or not such a cluster gas is the general feature which appears in other nuclear systems. In order to search for such the dilute cluster states, we studied the structure of excited states of ^{11}C and ^{11}B.

The present study has been motivated by the recent measurements of Gamov-Teller (GT) transitions ^{11}B$\rightarrow^{11}$C* with high energy resolutions[3, 4]. In the experiments, the GT transition strengths to the $3/2^-_3$ and the $5/2^-_2$ states were separately measured, and the transition to the ^{11}C$(3/2^-_3, 8.10$MeV) was found to be extremely weak compared with that to the ^{11}C$(5/2^-_2, 8.42$MeV) and also with those to other low-lying states. Abnormal features of the $3/2^-_3$ have been known also in the mirror nucleus ^{11}B. For example, the $3/2^-_3$ of ^{11}B has relatively weak $M1$ transitions into the lower states compared with strong transitions among other low-lying states. Another characteristic of the ^{11}B$(3/2^-_3)$ is the strong monopole transition observed by the recent experiments of the inelastic (d, d') scattering, where similarities of the ^{11}B$(3/2^-_3)$ with the ^{12}C(0^+_2) were suggested[5]. In the theoretical side, the structure of the ^{11}B$(3/2^-_3)$ state has been mysterious because this state can not be described by any models. No theoretical state can be assigned to the $3/2^-_3$ in shell model calculations[6, 7, 8] nor cluster model calculations[9]. These facts indicate that the $3/2^-_3$ of ^{11}B and ^{11}C may have an abnormal structure, and is a candidate of the dilute cluster state. On the other hand, the shell models succeeded to reproduce various properties of the low-lying negative-parity states with the excitation energy $E_x < 9$ MeV except for the $3/2^-_3$[8]. It suggests the possible coexistence of cluster states and non-cluster states in ^{11}B and ^{11}C.

In this paper, we study the negative-parity states of ^{11}B and ^{11}C based on the theoretical calculations of antisymmetrized molecular dynamics(AMD). We apply the method of variation after spin-parity projections in the AMD framework, which has been proved to be a powerful tool for studying excited states of light nuclei. We focus on the structure of the $3/2^-_3$ and the $5/2^-_2$ around $E_x = 8$ MeV, and show the similarity of the excited states of ^{11}B with those of ^{12}C.

The paper is organized as follows. First, we briefly explain the theoretical method in II, and then we show the calculated results comparing with the experimental data in III. In IV, the structure of excited states of ^{11}B is discussed, and their similarity with ^{12}C is shown. Finally, we give a summary in V.

II. FORMULATION

We perform the energy variation after spin parity projection(VAP) within the AMD model space, as was done in the previous studies[10, 11]. The detailed formulation of the AMD method for nuclear structure studies is described in [10, 11, 12, 13, 14]. In particular, the formulation of the present calculations is basically the same as that described in [10, 11, 15].

An AMD wave function is a Slater determinant of Gaussian wave packets;

$$\Phi_{\rm AMD}(\mathbf{Z}) = \frac{1}{\sqrt{A!}}\mathcal{A}\{\varphi_1, \varphi_2, ..., \varphi_A\}, \tag{1}$$

where the i-th single-particle wave function is written by a product of spatial(ϕ), intrinsic spin(χ) and isospin(τ) wave functions as,

$$\varphi_i = \phi_{\mathbf{X}_i}\chi_i\tau_i, \tag{2}$$

$$\phi_{\mathbf{X}_i}(\mathbf{r}_j) \propto \exp\{-\nu(\mathbf{r}_j - \frac{\mathbf{X}_i}{\sqrt{\nu}})^2\}, \tag{3}$$

$$\chi_i = (\frac{1}{2} + \xi_i)\chi_\uparrow + (\frac{1}{2} - \xi_i)\chi_\downarrow. \tag{4}$$

ϕ and χ are represented by complex variational parameters, X_{1i}, X_{2i}, X_{3i}, and ξ_i. The iso-spin function τ_i is fixed to be up(proton) or down(neutron). We use the fixed width parameter $\nu = 0.19$ fm^{-2}, which is chosen to be the optimum value for ^{11}B. Accordingly, an AMD wave function is expressed by a set of variational parameters, $\mathbf{Z} \equiv \{\mathbf{X}_1, \mathbf{X}_2, \cdots, \mathbf{X}_A, \xi_1, \xi_2, \cdots, \xi_A\}$.

For the lowest J^π state, we vary the parameters $\mathbf{X}_i$ and $\xi_i (i = 1 \sim A)$ to minimize the energy expectation value of the Hamiltonian, $\langle\Phi|H|\Phi\rangle/\langle\Phi|\Phi\rangle$, for the spin-parity projected AMD wave function; $\Phi = P^{J\pi}_{MK'}\Phi_{\rm AMD}(\mathbf{Z})$. Here, $P^{J\pi}_{MK'}$ is the spin-parity projection operator. Then we obtain the optimum solution of the parameter set; $\mathbf{Z}^{J\pi}_1$ for the lowest J^π state. The solution $\mathbf{Z}^{J\pi}_n$ for the n-th J^π state are calculated by varying $\mathbf{Z}$ so as to minimize the energy of the wave function;

$$|\Phi\rangle = |P^{J\pi}_{MK'}\Phi_{\rm AMD}(\mathbf{Z})\rangle - \sum_{k=1}^{n-1}|P^{J\pi}_{MK'}\Phi_{\rm AMD}(\mathbf{Z}^{J\pi}_k)\rangle\frac{\langle P^{J\pi}_{MK'}\Phi_{\rm AMD}(\mathbf{Z}^{J\pi}_k)||P^{J\pi}_{MK'}\Phi_{\rm AMD}(\mathbf{Z})\rangle}{\langle P^{J\pi}_{MK'}\Phi_{\rm AMD}(\mathbf{Z}^{J\pi}_k)|P^{J\pi}_{MK'}\Phi_{\rm AMD}(\mathbf{Z}^{J\pi}_k)\rangle}, \tag{5}$$

which is the orthogonal component to the lower states.

After the VAP calculations of the J^π_n states for various J, n and $\pi = \pm$, we obtained the optimum intrinsic states, $\Phi_{\rm AMD}(\mathbf{Z}^{J\pi}_n)$, which approximately describe the corresponding J^π_n states. In order to improve the wave functions, we superpose all the obtained AMD wave functions. Namely, we determine the final wave functions for the J^π_n states as,

$$|J^\pi_n\rangle = \sum_{i,K} c(J^\pi_n, i, K)|P^{J\pi}_{MK}\Phi_{\rm AMD}(\mathbf{Z}^{J_i\pi_i}_{k_i})\rangle, \tag{6}$$

where the coefficients $c(J^\pi_n, i, K)$ are determined by the diagonalization of the Hamiltonian and norm matrices. Here the number of the independent AMD wave functions, which are superposed in Eq.6, is that of the spin parity states $\{J^\pi_n\}$ calculated by the VAP. We calculate the expectation values for various observables with the $|J^\pi_n\rangle$ obtained after the diagonalization.

III. RESULTS

We adopt the same effective nuclear interaction as those used in Ref. [10], which consists of the central force, the spin-orbit force and the Coulomb force. The interaction parameters are slightly modified from the previous ones for better reproduction of the energy levels of ^{11}B and ^{11}C. Namely, the Bartlett, Heisenberg and Majorana parameters in the MV1 force are chosen to be $b = h = 0.25$ and $m = 0.62$, and the strengths of the spin-orbit force are $u_I = -u_{II} = 2800$ MeV.

The base AMD wave functions are obtained by the VAP for the ground and the excited states of ^{11}B. The number of the base AMD wave functions in the present calculations are 17. These independent AMD wave functions are superposed to calculate the final wave functions. In the calculations of the ^{11}C, we assume the mirror symmetry of the base AMD wave functions for simplicity. The coefficients of the base wave functions in the superposition are optimized for each system of ^{11}B and ^{11}C.

The energy levels of the negative parity states in ^{11}B are shown in Fig. 1. In the results, we obtain the $3/2^-_3$ and the $5/2^-_2$ at about $E_x = 10$ MeV. We can assign the obtained $3/2^-_3$ and $5/2^-_2$ to the observed $3/2^-_3 (E_x = 8.56$ MeV) and $5/2^-_2 (E_x = 8.92$ MeV) due to the good agreements of transition strengths between theory and experimental data as shown later, though the excitation energies are overestimated by the present calculations.

The GT transition strengths from the $^{11}\mathrm{B}_{\rm g.s.}$ to $^{11}\mathrm{C}^*$, the $M1$ and $E2$ transition strengths in ^{11}B are shown in tables I, II and III,respectively. The calculated values for these transitions are in good agreements with the observed

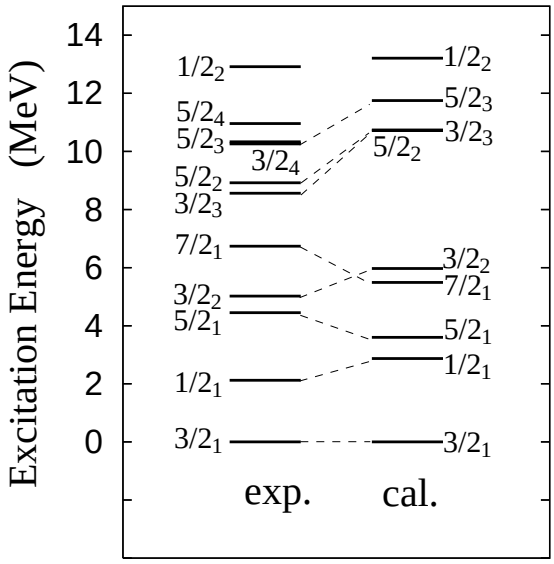

FIG. 1: Energy levels of the negative-parity states of ^{11}B.

values. The B(GT) for the transitions to the ^{11}C$^*(3/2_3^-)$ and the ^{11}C$^*(5/2^-2)$ at $E_x \sim 8$ MeV were recently measured by charge exchange reactions[3, 4], and it was found that B(GT;^{11}B$\rightarrow^{11}$C$(3/2_3^-)$) is abnormally small while B(GT;^{11}B$\rightarrow^{11}$C$(5/2_2^-)$) is as large as those for other low-lying states of ^{11}C. The present result well describes the small B(GT) for the $3/2_3^-$ state because it has a well developed 2α+^{3}He cluster structure, and hence, the structure of the daughter state much differs from the normal structure of the parent state, ^{11}B$_{\rm g.s.}$. Due to the same reason, the $M1$ transitions from the ^{11}B$(3/2_3^-)$ to the low-lying states are generally weak compared with other $M1$ transitions among the low-lying states. On the other hand, since the $5/2_2^-$ has no cluster structure, the B(GT) for the ^{11}C$^*(5/2_2^-)$ and the $B(M1)$ for the ^{11}B$^*(5/2_2^-)$ are as large as those for the other low-lying states in the theoretical results. This is consistent with the experimental data. We also show the theoretical B(GT) calculated by the no-core shell model(NCSM)[8] in table I. The strengths of the GT transitions to ^{11}C* are reproduced also by NCSM except for the transition to the ^{11}C$^*(3/2_3^-)$. In the NCSM, the $3/2_3^-$ can not be described because the limited model space in the shell model is not suitable to describe cluster states with the spatial development.

In the recent experiments of the inelastic (d, d') scattering [5], it has been found that the iso-scalar monopole transition for $3/2_1^- \rightarrow 3/2_3^-$ is as strong as $B(E0; IS) = 94 \pm 16$ fm^4. The calculated strength for this inelastic transition is $B(E0; IS) = 94$ fm^4, which well agrees with the experimental data.

IV. DISCUSSIONS

In the present calculations of ^{11}B and ^{11}C, we found that the $3/2_3^-$ states are the well developed three-center cluster states like $2\alpha + t$ and 2α+^{3}He. We consider that these states are the candidates of the cluster gas state, which has an analogy to the 3α gas state proposed in the ^{12}C(0_2^+). On the other hand, the $5/2_2^-$ at almost the same excitation energy as the $3/2_3^-$ is the non-cluster state. In this section, we theoretically investigate the structure of ^{11}B while focusing on cluster aspect, and show the analogy of the excited states of ^{11}B with those of ^{12}C.

A. Intrinsic structure

As explained in II, by performing the VAP calculations we obtained the optimum intrinsic states, $\Phi_{\rm AMD}(\mathbf{Z}_n^{J\pi})$. Although the final wave function $|J_n^\pi\rangle$ is expressed by the superposition of all the obtained AMD wave functions as 6, the spin-parity eigen state $|P^{J\pi}_{MK}\Phi_{\rm AMD}(\mathbf{Z}_n^{J\pi})\rangle$ projected from the single AMD wave function is the dominant component of the $|J_n^\pi\rangle$ with the amplitude of more than 70% in most cases except for the $3/2_3^-$. In the case $3/2_3^-$, since the amplitude is distributed into various AMD wave functions, the amplitude of the dominant component

TABLE I: Comparison of the GT transition strengths, the binding energies, Q-moments, μ-moments and $2\alpha - t$ threshold between present results and the experimental data. The theoretical values obtained by the no-core shell model calculation with AV8'+TM'(99) [8] are also shown. The experimental data are taken from Ref.[4].

	exp.	AMD	NCSM
B(GT;^{11}B$\to^{11}$C$(3/2^-_1)$)	0.345(8)	0.40	0.315
B(GT;^{11}B$\to^{11}$C$(1/2^-_1)$)	0.440(22)	0.43	0.591
B(GT;^{11}B$\to^{11}$C$(5/2^-_1)$)	0.526(27)	0.70	0.517
B(GT;^{11}B$\to^{11}$C$(3/2^-_2)$)	0.525(27)	0.67	0.741
B(GT;^{11}B$\to^{11}$C$(3/2^-_3)$)	0.005(2)	0.02	
B(GT;^{11}B$\to^{11}$C$(5/2^-_2)$)	0.461(23)	0.56	0.625
B.E.(^{11}B$_{\rm g.s.}$) [MeV]	76.205	72.8	73.338
$\mu(^{11}\mathrm{B}_{\rm g.s.})$ [μ_N^2]	+2.689	+2.3	+2.176
$Q(^{11}\mathrm{B}_{\rm g.s.})$ [e fm^2]	+4.065(26)	+4.7	+2.920
B.E.(^{11}C$_{\rm g.s.}$) [MeV]	73.440	70.4	70.618
$\mu(^{11}\mathrm{C}_{\rm g.s.})$ [μ_N^2]	−0.964	−0.6	−0.460
$Q(^{11}\mathrm{C}_{\rm g.s.})$ [e fm^2]	+3.327(24)	+3.8	+2.363
$2\alpha + t$ threshold [MeV]	65.07	70.6	

TABLE II: $M1$ transition strengths in ^{11}B. The theoretical values were calculated by the AMD (VAP) method.

		$B(M1; J_i \to J_f)$ μ_N^2	
J_i	J_f	exp.	theor.
$1/2^-_1$	$3/2^-_1$	1.07 (0.07)	1.2
$5/2^-_1$	$3/2^-_1$	0.52 (0.02)	0.72
$3/2^-_2$	$3/2^-_1$	1.13 (0.04)	1.2
$3/2^-_2$	$1/2^-_1$	0.98 (0.04)	1.0
$7/2^-_1$	$5/2^-_1$	0.006 (0.002)	0.03
$3/2^-_3$	$3/2^-_1$	0.072 (0.007)	0.07
$3/2^-_3$	$1/2^-_1$	0.091 (0.009)	0.16
$3/2^-_3$	$5/2^-_1$	0.057 (0.013)	0.04
$3/2^-_3$	$3/2^-_2$	0.163 (0.023)	0.28
$5/2^-_2$	$3/2^-_1$	0.50 (0.02)	0.45
$5/2^-_2$	$5/2^-_1$	0.21 (0.02)	0.04

$|P^{3/2^-}_{MK}\Phi_{\rm AMD}(\mathbf{Z}_3^{3/2^-})\rangle$ in the $|3/2^-_3\rangle$ is reduced to 50%. Here we regard the obtained $\Phi_{\rm AMD}(\mathbf{Z}_n^{J\pi})$ written by the single Slater determinant as the approximate intrinsic state of the corresponding J^π_n state, and discuss the intrinsic structure.

In Fig. 2, we display the density distribution of the excited states of ^{11}B. The matter density of the intrinsic wave functions $\Phi_{\rm AMD}(\mathbf{Z}_n^{J\pi})$ is shown. As shown in the density, the ground state($3/2^-_1$) has no cluster structure, while the $3/2^-_2$ state has a structure with cluster cores. Since the spatial development of the clustering is not remarkable, the $3/2^-_2$ state is considered to be the $SU(3)$-limit cluster state. Most striking thing is that the spatially developed cluster structure of $2\alpha + t$ appears in the $3/2^-_3$ state. On the other hand, the $5/2^-_2$ state has no cluster structure though this state appears at almost the same excitation energy as the $3/2^-_3$ state with the developed cluster structure. In higher excited state, we found a somewhat linear-like $2\alpha + t$ cluster structure in the $1/2^-_2$. The predicted $1/2^-_2$ state should be assigned to a $1/2^-, T = 1/2$ state, however, the corresponding state has not been observed yet.

Let us show similarities of the cluster features seen in the intrinsic structure of ^{11}B with those of ^{12}C. We compare the present AMD results with those of ^{12}C in Ref.[15]. Then we find a good correspondence of the intrinsic structure between ^{11}B and ^{12}C. As shown in Fig.2, the ground states in both nuclei has no remarkable cluster structure due to the nature of the $p_{3/2}$ sub-shell closure. The cluster core structure in the $^{11}\mathrm{B}(3/2^-_2)$ state is similar to that of the $^{12}\mathrm{C}(2^+_1)$. Both the states show the three-center cluster core structure but the spatial development is not remarkable. It means that the $^{11}\mathrm{B}(3/2^-_2)$ and the $^{12}\mathrm{C}(2^+_1)$ can be practically dominated by the $SU(3)$-limit cluster states of $2\alpha+t$ and 3α, respectively. The spatially developed $2\alpha+t$ clustering in the $^{11}\mathrm{B}(3/2^-_3)$ is similar to the developed 3α clustering in the $^{12}\mathrm{C}(0^+_2)$. The details are discussed later. The linear-like structure in the $^{11}\mathrm{B}(1/2^-_2)$ is associated with that of the

TABLE III: The quadrupole transition strengths in ^{11}B. The present results of the $B(E2)$, M_p and M_n are shown with the experimental values of $B(E2)$[16].

J_i	J_f	exp.	theor.		
		$B(E2)$ e^2 fm^4	$B(E2)$ e^2 fm^4	M_p e fm^2	M_n e fm^2
$1/2^-_1$	$3/2^-_1$		4.5	3.0	4.0
$5/2^-_1$	$3/2^-_1$	14(3)	12.8	8.8	7.5
$3/2^-_2$	$3/2^-_1$		0.0	0.3	2.7
$7/2^-_1$	$3/2^-_1$	1.9(0.4)	1.8	3.8	7.9
$3/2^-_3$	$3/2^-_1$		0.8	1.8	2.8
$5/2^-_2$	$3/2^-_1$	1.0(0.7)	0.1	0.8	0.9
$5/2^-_3$	$3/2^-_1$		0.7	2.1	1.2

^{12}C(0^+_3) and ^{12}C(1^-_1) states. Although the structure of the ^{12}C(0^+_3) is not experimentally and theoretically clarified yet, the linear-like 3α structure in ^{12}C was predicted by the generator coordinate method(GCM) calculation[17] and also by the fermionic molecular dynamics[18] as well as the AMD. The $5/2^-_2$ has no cluster structure because this state appears due to the intrinsic spin excitation, which causes the breaking of clusters. The situation is similar to the case of ^{12}C(1^+_1).

As mentioned before, the ^{11}C($3/2^-_3$, 8.10 MeV) and ^{11}B($3/2^-_3$, 8.65 MeV) have the abnormally small B(GT) and $B(M1)$ compared with the other low-lying states in $E_x \leq 9$ MeV. The quenching of GT and $M1$ transitions for the $3/2^-_3$ states can be described by the above-mentioned exotic structure. Namely, since the ^{11}C($3/2^-_3$) and the ^{11}B($3/2^-_3$) exhibit the well-developed 2α+^{3}He and $2\alpha+t$ clustering, they have small transition overlap with the other normal low-lying states.

B. Dilute cluster states in the $3/2^-_3$

By analyzing the obtained wave functions, we found that the ^{11}B($3/2^-_3$) is a three-center cluster state with the spatially developed $2\alpha+t$ clustering. The clustering features of the ^{11}B($3/2^-_3$) and the ^{11}C($3/2^-_3$) are very similar to those of ^{12}C(0^+_2, 7.65 MeV), which is known to be a dilute gas-like 3α state. Therefore, we consider that the ^{11}C($3/2^-_3$, 8.10 MeV) and the ^{11}B($3/2^-_3$,8.56 MeV) are the candidates of the dilute gas-like cluster states with 2α+^{3}He and $2\alpha+t$, respectively. The similarity of the ^{11}B($3/2^-_3$) with the ^{12}C(0^+_2) has been suggested in Ref.[5], where the experimental data of the (d,d') scattering have been analyzed. We here theoretically discuss the similarity between the ^{11}B($3/2^-_3$) and the ^{12}C(0^+_2) by comparing the wave functions of ^{11}B and those of ^{12}C obtained by the AMD as same as the present work[15].

In order to see the diluteness of the cluster states, first we plot the matter density $\rho(r)$ as a function of the radius r in Fig. 3. In the ground states of ^{11}B and ^{12}C, the density distributes in the small r region because of their compact structures. On the other hand, the density in the ^{11}B($3/2^-_3$) state is about a half of the normal density at the center and has a tail in the outer region due to the spatial development of clusters. The density curve of the ^{11}B($3/2^-_3$) is similar to that of the ^{12}C(0^+_2) though the outer tail is less remarkable than the ^{12}C(0^+_2). Next we show the matter root-mean-square radii of the ground and the excited states of ^{11}B and ^{12}C in Table IV. In ^{12}C, the 0^+_2 has a large radius. The calculated value of the 0^+_2 is 3.3 fm in the AMD calculations, while those obtained by the RGM calculations[19] and the α condensate wave functions[2] are 3.5 fm and 3.8 fm, respectively. The smaller theoretical radius in the present method is considered to be because of the limited number of the base wave functions. In ^{11}B, the radius of the $3/2^-_3$ state is remarkably large compared with the size of the ground state. Considering the large radius and the density tail in the outer region, we can say that the $3/2^-_3$ state shows the nature of a dilute cluster state.

In order to give more quantitative discussions of the spatial development of clusters, we examine the expectation values of the harmonic oscillator(H.O.) quanta for protons and neutrons in table IV. For the width parameters of the H.O., we use the same width of the Gaussian wave packets adopted in the AMD wave function. The values ΔQ are defined by subtracting the minimum oscillator quanta from the expectation values of the principal quantum number of H.O.,

$$\Delta Q \equiv \langle a^\dagger a \rangle - Q_{\rm min}, \tag{7}$$

where $Q_{\rm min}$ is 3(4) and 4(4) for protons(neutrons) of ^{11}B and ^{12}C, respectively. The expectation values of the oscillator quanta indicate the higher shell components in terms of the H.O. shell model. It is generally enhanced when

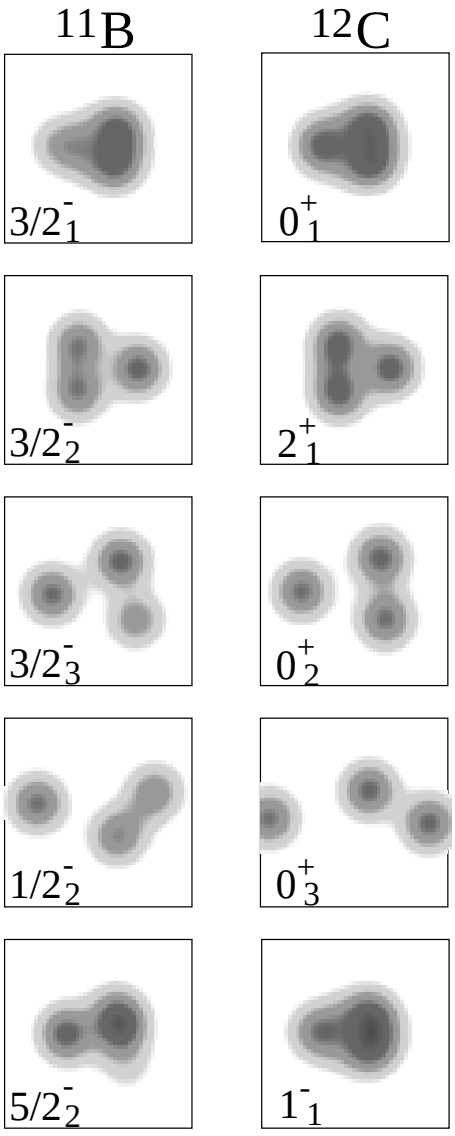

FIG. 2: Density distribution of the ground and excited states in ^{11}B and ^{12}C. The density of the dominant AMD wave function of each state is shown.

the clustering spatially develops, because it necessarily increases the higher shell components. In the ^{12}C(0^+_2) and the ^{11}B($3/2^-_3$), the large ΔQ values are caused by the developed three-center cluster structure. Such the higher shell components due to the cluster correlation in the developed cluster states can not be treated in the truncated space of shell model. This is the reason why the shell model calculations fail to describe the ^{12}C(0^+_2) and the ^{11}B($3/2^-_3$). On the other hand, the ΔQ values in the ^{11}B($3/2^-_2$) are rather small compared with those of the $3/2^-_3$. It means that the major component of the $3/2^-_2$ is the $0\hbar\omega$ configuration. Since it has a compact state with cluster cores as shown in Fig. 2, this state is interpreted to be almost the SU(3)-limit cluster state.

The similarity between the ^{11}B($3/2^-_3$) and the ^{12}C(0^+_2) has been suggested in Ref.[3, 5], where the multipole decomposition analysis of the inelastic (d, d') scattering has been performed. The remarkable strengths of inelastic monopole transitions are the characteristics of these states. Figure 4. shows the calculated electron form factor for the monopole transitions, ^{12}C($0^+_1 \to 0^+_2$), ^{11}B($3/2^-_1 \to 3/2^-_2$) and ^{11}B($3/2^-_1 \to 3/2^-_3$). The profile and the absolute value of the form factor are similar between the ^{11}B($3/2^-_1 \to 3/2^-_3$) and the ^{12}C($0^+_1 \to 0^+_2$), while the form factor for the ^{11}B($3/2^-_1 \to 3/2^-_2$) is more than factor 10^2 smaller. This is consistent with the experimental results of the (d, d') scattering[3, 5].

As mentioned above, we can see the developed cluster structure with dilute density in the ^{11}B($3/2^-_3$) as well as the

TABLE IV: Matter root-mean-square radii(r.m.s.r.) and expectation values of the harmonic oscillator quanta for protons(ΔQ_p) and neutrons(ΔQ_n). The values of ΔQ are defined by subtracting the minimum oscillator quanta. See the details in the text. The expectation values of the squared intrinsic spin for neutrons $\langle \mathbf{S}_n^2 \rangle$ are also listed. The observed r.m.s.r. of the ^{12}C(0_1^+) is estimated to be $2.32 - 2.33$ fm by the electron scattering data.

	r.m.s.r. (fm)	ΔQ_p	ΔQ_n	$\langle \mathbf{S}_n^2 \rangle$
^{11}B($3/2_1^-$)	2.5	0.3	0.4	0.7
^{11}B($3/2_2^-$)	2.7	0.9	1.1	0.2
^{11}B($3/2_3^-$)	3.0	2.0	2.6	0.4
^{11}B($1/2_1^-$)	2.7	0.7	0.8	0.3
^{11}B($1/2_2^-$)	3.1	3.0	3.6	0.3
^{11}B($5/2_1^-$)	2.6	0.5	0.7	0.5
^{11}B($5/2_2^-$)	2.6	0.5	0.7	1.3
^{11}B($5/2_3^-$)	2.7	0.7	0.9	0.8
^{12}C(0_1^+)	2.5	0.4	0.4	0.6
^{12}C(0_2^+)	3.3	4.4	4.3	0.3
^{12}C(0_3^+)	4.0	10.0	9.9	0.1
^{12}C(2_1^+)	2.7	0.8	0.8	0.2
^{12}C(1_1^+)	2.5	0.2	0.2	1.4

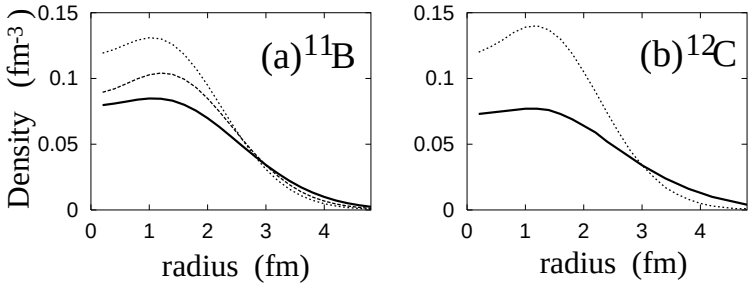

FIG. 3: Point matter density of (a) the $3/2_1^-$(dotted), $3/2_2^-$(dashed) and $3/2_3^-$(solid) states of ^{11}B, and (b) the 0_1^+(dotted) and 0_2^+(solid) of ^{12}C.

^{12}C(0_2^+). The ^{12}C(0_2^+) is interpreted as a cluster gas state, where 3 α clusters are rather freely moving[1, 2]. Here "a cluster gas" means the well developed cluster state with dilute density, where the clusters are freely moving in terms of the weak coupling picture. Such the gas-like nature is reflected not only in the dilute density but also in the fragmentation of the amplitudes in the AMD model space. Let us remind the reader that a base AMD wave function is expressed by a Slater determinant. If the cluster state is written by an AMD wave function, it has a certain spatial configuration of the cluster centers like a single Brink-type cluster wave function[22]. On the contrary, when the state has a cluster gas-like feature, its wave function is written by a superposition of various AMD wave functions with different configurations of cluster centers. As a results, the cluster gas state is not dominated by a single AMD wave function, but the amplitudes distribute in various base wave functions. Actually in the ^{12}C(0_2^+), the amplitude of the $|P^{0+}_{MK}\Phi_{\rm AMD}(\mathbf{Z}_2^{0+})\rangle$ is reduced to about 50% because of the cluster gas nature as discussed in Ref.[15]. Similarly, in the case of ^{11}B($3/2_3^-$), the amplitude of the dominant component is only 50%, while those for the ^{11}B($3/2_1^-$) and ^{11}B($3/2_2^-$) are more than 90%. This indicates the gas-like nature of $2\alpha + t$ cluster in the ^{11}B($3/2_3^-$) as well as the 3α cluster in the ^{12}C(0_2^+).

Considering the smaller radius of the ^{11}B($3/2_3^-$) than the ^{12}C(0_2^+), the cluster gas-like nature in the ^{11}B($3/2_3^-$) is not so remarkable as that in the ^{12}C(0_2^+). We consider the reasons for the less gas-like nature in the ^{11}B($3/2_3^-$) as follows. Firstly, the inter-cluster potential is more attractive in the $\alpha - t$ channel than the $\alpha - \alpha$ channel. This is already known in the comparison of the binding energy between ^{7}Li and ^{8}Be. The origin is that the repulsive Pauli effect is smaller in the $\alpha - t$ than the $\alpha - \alpha$. Second, from the natural extension of the the ground state properties of ^{7}Li and ^{8}Be it is expected that the triton motion may have the orbital angular-momentum $L = 1$ while the motion of the α clusters has $L = 0$. The $L = 1$ should be less favored to form a dilute cluster gas state than the $L = 0$. Thirdly, it might be important that the symmetry of three clusters is not good in the $2\alpha + t$ system as the 3α system. Because of the symmetry of 3 α orbits, the ^{12}C(0_2^+) state is understood as the α condensate state as argued in Refs.[1, 2, 23, 24].

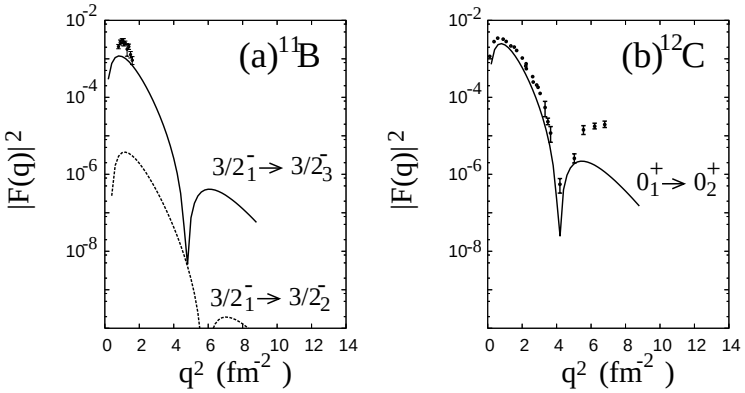

FIG. 4: Squared inelastic form factors for the electron scattering on (a)^{11}B and (b)^{12}C. The experimental form factors for the transitions to ^{11}B($3/2^-, 8.56$MeV) and ^{12}C(0^+_2) are taken from [20] and [21], respectively. The lines are the calculated form factors of the $E0$ components.

However, it is not easy to define the Bosonic behavior and to discuss the condensation in the $2\alpha + t$ system, which contains only two identical bosons.

In the stabilizing mechanism of the dilute cluster states, one of the keys preventing the states from shrinking is the orthogonality to the compact states in the lower energy region. In both cases of ^{12}C and ^{11}B, there exist the lower states with the compact cluster components. In the higher cluster states, the cluster distribution avoids the compact inner region and must spread out to satisfy the orthogonality to the lower states. It is interesting that the the number of the lower compact states is one(0^+_1) in ^{12}C and it is two($3/2^-_1$,$3/2^-_2$) in case of ^{11}B, which is just the number of the low-lying states described by the $0\hbar\omega$ configurations. This is the reason why the dilute cluster state appears in the *third* $3/2^-$ state in the ^{11}B system.

The diluteness of the cluster states should be sensitive also to the relative energy against the threshold energy of the corresponding cluster channel. In the present results, the threshold energy for the three-body cluster breakup is not reproduced. In order to check the dependence of the relative energy of the excited state to the threshold, we vary the relative energy by changing the interaction parameters, and found that the structure of the excited states are qualitatively unchanged. It means that the present results are not sensitive to the relative position of the threshold. It is because the present framework is a kind of bound state approximation. Since the number of the base wave functions is limited, the long tail part of the inter-cluster motion may not be enough taken into account, and therefore the description of the detailed resonant behavior is insufficient in the present framework. In fact, the AMD calculations give the smaller radius of the ^{12}C(0^+_2) than that obtained by the 3α cluster models. However, we should stress that the features of 3α system obtained by the present method are qualitatively similar to those of the 3α-GCM calculations by Uegaki *et al.*[17], and also consistent with the 3α model of orthogonal condition method(OCM) with the complex scaling method(CSM)[25] where the resonant behavior was appropriately treated. It implies that the present results are useful for qualitative discussions, though the long tail part of the inter-cluster motion and its boundary conditions should be carefully treated for further quantitative study.

We should comment that the loosely bound cluster states have been predicted by Nishioka *et al.* with a $2\alpha+t$-OCM cluster model[9]. However, they could not assign the $3/2^-_3$ state because the reproduction of the energy spectra in the low-energy region was poor in the cluster model space.

C. Intrinsic spin excitation

In the ideal $2\alpha+t$ and 3α cluster states, the expectation values of the squared total intrinsic spin for neutrons($\langle \mathbf{S}^2_n \rangle$) should be zero, because spin-up and spin-down neutrons couple to be spin-zero pairs. In ^{11}B and ^{12}C, non-zero values of $\langle \mathbf{S}^2_n \rangle$ is caused by the component of the cluster breaking. We show the values of $\langle \mathbf{S}^2_n \rangle$ in ^{11}B and also those in ^{12}C in table IV. The $\langle \mathbf{S}^2_n \rangle$ values are small in the cluster states such as the ^{11}B($3/2^-_2$), ^{11}B($3/2^-_3$) and ^{11}B($1/2^-_2$). while that of the ^{11}B$_{\rm g.s.}$ is significantly large as $\langle \mathbf{S}^2_n \rangle = 0.7$ due to the component of the $p_{3/2}$ sub-shell closure as well as that of the ^{12}C$_{\rm g.s.}$. An interesting point is the large value, $\langle \mathbf{S}^2_n \rangle = 1.3$, in the ^{11}B($5/2^-_2$). This means that the $5/2^-_2$ state is characterized by the intrinsic spin excitation of neutrons within the p-shell. This feature well corresponds to the structure of the ^{12}C(1^+_1), which is assigned to the observed 1^+_1(12.7 MeV) state. In the comparison of the experimental excitation energies between ^{11}B($5/2^-_2$) and ^{12}C(1^+_1) with the intrinsic spin excitation, it is interesting that

the ^{11}B($5/2^-_2$, 8.92 MeV) appears in the low-energy region and almost degenerate with the cluster gas-like ^{11}B($3/2^-_3$, 8.56 MeV), while the ^{12}C(1^+_1, 12.7 MeV) exists at much higher excitation energy than the ^{12}C(0^+_2, 7.6 MeV). It implies that the intrinsic spin excitation easily occurs in ^{11}B than the ^{12}C, and that the excitation energy of the intrinsic spin excitation is almost the same as that of the cluster excitation in ^{11}B.

V. SUMMARY

We studied the negative-parity states in ^{11}B and ^{11}C based on the theoretical calculations of antisymmetrized molecular dynamics(AMD). It is concluded that various types of cluster states appear in the excited states of ^{11}B and ^{11}C. Recent experimental data of GT transition strengths for the $3/2^-_3$ and the $5/2^-_2$ states at $E_x \sim 8$ MeV are well reproduced by the cluster state and the non-cluster state, respectively. It was found that the excitation energy of the intrinsic spin excitation is almost the same as that of the cluster excitation in ^{11}B. We compared the cluster aspect in the excited states of ^{11}B with that of ^{12}C, and showed a good similarity between the $2\alpha + t$ and 3α systems.

We succeeded to describe the ^{11}B($3/2^-_3$, 8.56 MeV) and ^{11}C($3/2^-_3$, 8.10 MeV) states, which have not been reproduced by any other models. For the assignment of the theoretical states to the observed ones, it is essential to systematically describe the properties of the coexisting cluster and non-cluster states in ^{11}C and ^{11}B. One of the new revelations in the present work is that ^{11}C($3/2^-_3$) and ^{11}B($3/2^-_3$) are the well developed cluster states of 2α+^{3}He and $2\alpha + t$ with dilute density, respectively. The features of these dilute cluster states in ^{11}C and ^{11}B are similar to those of the 0^+_2 state of ^{12}C, which is understood to be a cluster gas of weakly interacting 3α particles.

Since the present framework is a kind of bound state approximation, the description of resonant behavior is not sufficient. The boundary conditions of the inter-cluster motion should be taken into account more carefully in more detailed investigations of the developed cluster states.

Acknowledgments

The author would like to thank Prof. Schuck, Prof. Kawabata and the member of the "Research Project for Study of Unstable Nuclei from Nuclear Cluster Aspects" sponsored by Institute of Physical and Chemical Research (RIKEN) for many discussions. The computational calculations in this work were performed by the Supercomputer Projects of High Energy Accelerator Research Organization(KEK) and also the super computers of YITP. This work was supported by Japan Society for the Promotion of Science and a Grant-in-Aid for Scientific Research of the Japan Ministry of Education, Science and Culture. The work was partially performed in the "Research Project for Study of Unstable Nuclei from Nuclear Cluster Aspects" sponsored by Institute of Physical and Chemical Research (RIKEN).

[1] A. Tohsaki, H. Horiuchi, P. Schuck and G. Röpke, Phys. Rev. Lett. **87**, 192501 (2001).
[2] Y. Funaki, A. Tohsaki, H. Horiuchi, P. Schuck and G. Röpke, Phys. Rev. C **67**, 051306(R) (2003).
[3] T. Kawabata *et al.*, Phys. Rev. C **70**, 034318 (2004).
[4] Y. Fujita et al., Phys. Rev. C **70**, 011306(R) (2004).
[5] T. Kawabata *et al.*, nucl-ex/0512040.
[6] S. Cohen and D. Kurath, Nucl.Phys. 73, 1 (1965).
[7] J. M. G. Gomez, J. C. Perez Cerdan and C.Prieto, Nucl. Phys. **A551**, 451 (1993).
[8] P. Navratil and W. E. Ormand, Phys. Rev. C **68**, 034305 (2003).
[9] H. Nishioka, S. Saito and M. Yasuno, Prog. Theor. Phys. **62** 424 (1979).
[10] Y. Kanada-En'yo, Phys. Rev. Lett. **81**, 5291 (1998).
[11] Y. Kanada-En'yo, H. Horiuchi and A. Doté, Phys. Rev. C **60**, 064304 (1999).
[12] Y. Kanada-En'yo, H. Horiuchi and A. Ono, Phys. Rev. C **52**, 628 (1995); Y. Kanada-En'yo and H. Horiuchi, Phys. Rev. C **52**, 647 (1995).
[13] Y. Kanada-En'yo and H. Horiuchi, Prog. Theor. Phys. Suppl.**142**, 205 (2001).
[14] Y. Kanada-En'yo, M. Kimura and H. Horiuchi, Comptes rendus Physique Vol.4, 497 (2003).
[15] Y. Kanada-En'yo, nucl-th/0605047.
[16] F. Ajzenberg-Selove, Nucl. Phys. A506, 1 (1990).
[17] E. Uegaki, S. Okabe, Y. Abe and H. Tanaka, Prog. Theor. Phys. **57**, 1262 (1977). E. Uegaki, Y. Abe, S. Okabe and H. Tanaka, Prog. Theor. Phys. **59**, 1031 (1978); **62**, 1621 (1979).
[18] T. Neff and H. Feldmeier, Nucl. Phys. **A738**, 357 (2004).
[19] Y. Fukushima and M. Kamimura, *Proc. Int. Conf. on Nuclear Structure, Tokyo, 1977, edited by T. Marumori*[J. Phys. Soc. Jpn. **44**, 225(1978); M. Kamimura, Nucl. Phys. **A351**, 456 (1981).

[20] V.N.Polishchuk, N.G.Shevchenko, N.G.Afanasev, A.Y.Buki, A.A.Khomich, Sov. J. Nucl. Phys. **29**, 297 (1979).
[21] I. Sick and J. S. McCarthy, Nucl. Phys. **A150**, 631 (1970); A. Nakada, Y. Torizuka and Y. Horikawa, Phys. Rev. Lett. **27**, 745 (1971); and 1102 (Erratum); P. Strehl and Th. H. Schucan, Phys. Lett. **27B**, 641 (1968).
[22] D.M. Brink, *Proceedings of the International School of Physics "Enrico Fermi"*, Varenna, 1965, Course 36, Ed. by C.Bloch (Academic Press, New York 1966)
[23] T. Yamada and P. Schuck, Phys. Rev. C **69**, 024309 (2004).
[24] H. Matsumura and Y. Suzuki, Nucl. Phys. **A739**, 238 (2004).
[25] C. Kurokawa and K. Kato, Nucl. Phys. **A738**, 455 (2004).